PHYSICAL REVIEW B VOLUME 24, NUMBER 12 15 DECEMBER 1981

Structure of the initial stages of oxidation of Al{111} surfaces from low-energy-electron diffraction and Auger electron spectroscopy

F. Soria
Laboratorio de Lámina Delgada, Instituto de Fisica de Materiales, Serrano 144, Madrid-6, Spain and Departamento de Física Fundamental, Universidad Autónoma de Madrid, Cantoblanco, Madrid-34, Spain*

V. Martínez
Centro de Investigación, Universidad Autónoma de Madrid—International Business Machines, Apartado 179, Madrid-1, Spain

M. C. Muñoz and J. L. Sacedón
Laboratorio de Lámina Delgada, Instituto de Física de Materiales, Serrano 144, Madrid-6, Spain
(Received 3 June 1981)

The structure of the initial stages of oxidation of Al{111} surfaces has been determined by low-energy-electron diffraction (LEED) and Auger-electron-spectroscopy (AES) measurements. The oxidation process can be described by a four-stage mechanism depending on the oxygen exposure: 0—30 L; 30—100 L; 100—200 L; and 200 onwards. At the end of the first stage, the transition density of states (TDOS) obtained by self-deconvolution of the Al{111}—25-L RT O_2-exposure $L_{2,3}VV$ AES spectra and comparison with theoretical calculations of the DOS for this coverage show that the oxygen atoms occupy the fcc threefold hollows in an underlayer configuration, with an interplanar distance $d_{12}=0.0-0.5$ Å. At 100-L RT O_2 exposure, AES and LEED indicate the formation of a complete Al{111} 1×1-O overlayer structure with the oxygen atoms occupying the fcc threefold hollows at $d_{12}=0.73\pm0.05$ Å. At 150 L, $d_{12}=0.80\pm0.03$ Å for the same Al{111} 1×1-O structure. These LEED values solve the discrepancy with the surface-extended x-ray-absorption fine-structure measurements, and suggest the need for a revision of interplanar distances previously determined by LEED for oxygen-metal structures.

I. INTRODUCTION

The chemisorption of simple gases on free-electron metals has been of great theoretical and experimental interest during the past years for its importance in the understanding of catalytic reactions and oxidation processes. In particular, the clean surfaces of Al{100}, Al{110}, and Al{111} and their interactions with oxygen have been extensively studied. However, while adsorption on Al{100} and Al{110} seems to be well understood,[1-3] adsorption on Al{111} surfaces still presents many controversial issues. Several models have been proposed to explain the position of the chemisorbed oxygen layer with respect to the Al{111} surface, namely, ordered overlayer formation,[3-8] random overlayer,[9-10] or a combination of underlayer and overlayer in a dynamical process.[12-14]

Interplanar distances have been measured using several techniques, most frequently by LEED and surface-extended x-ray-absorption fine-structure techniques (SEXAFS). The results obtained are rather sparse, and markedly different for the clean Al{111} surfaces.[15-18] Two independent LEED studies with two different experimental data sets give identical results.[15-17] Jona *et al.*[16] using the quantitative R-factor technique found an expansion of the first Al layer of 2.2% ($d_{12}=2.39\pm0.03$ Å) with an inner potential $V_0=8.7\pm0.6$ eV. Yu *et al.*[17] by visual evaluation found the first Al layer to be expanded about 2.37 Å (2.338 Å $\leq d_{12} \leq$ 2.40 Å), with an inner potential $V_0=8.5\pm2$ eV. On the contrary, SEXAFS[18] gives for the interplanar distance between the first and second layer, the value $d_{12}=2.15\pm0.06$ Å which represents a contraction of 8.1% of the bulk interlayer spacing along ⟨111⟩ (2.338 Å).

For the interplanar distance between the chemisorbed oxygen layer and the Al{111} surface d_{12}, the discrepancy persists. Three independent LEED studies[5,17,19] give the following results: Martinson *et al.*,[5] $d_{12}=1.33\pm0.08$ Å; Yu *et al.*,[17] $d_{12}=1.46\pm0.05$ Å; and Payling and Ramsey,[19] $d_{12}=1.54$ Å. These distances correspond to oxygen radii of 0.69, 0.77, and 0.83 Å, respectively, and their mean value of 0.76 Å falls inside the values found for oxygen adsorption on other metals (Ni,Cu,Fe,Co), 0.66 Å to 0.78 Å. Again, SEXAFS[20,21] measurements are quite different, giving $d_{12}=0.7$ $(+0.1, -0.15)$ Å, which corresponds to an oxygen radius of about 0.40 Å, almost half of the LEED average value.

Theoretical calculations for the O-Al{111} system present the same discrepancies. Lang *et al.*[22–24] give for the interplanar distance between the oxygen-chemisorbed layer and the first Al layer, $d_{12}=1.75$ Å or $d_{12}=1.32$ Å. These distances compare well with the values found by LEED. Salahub *et al.*[25] place the oxygen atoms on the threefold fcc hollows of the Al{111} surface, and find two possible d_{12} values. $d_{12}=0.0$ Å at low oxygen exposures (≤ 0.16 monolayers) with an Al{111} surface lattice expanded by 10%, and $d_{12}=0.53-1.06$ Å at higher exposures. This second value is in agreement with SEXAFS measurements.

Unfortunately, not only do two different techniques give different results, but even worse, different authors utilizing the same techniques[3,8,9] find different results. Moreover, experimental conditions such as working pressure influence the results obtained.[12] That is, the results of an oxygen adsorption at 10^{-8} Torr are not necessarily identical to those obtained for the same amount of gas at, say, 10^{-7} Torr.

In this paper we try to clarify the initial adsorption of oxygen on clean Al{111} surfaces at an oxygen pressure of 1×10^{-7} Torr (pressure of the majority of published works). We have used Auger electron spectroscopy (AES) and LEED as basic sources of experimental data. AES $L_{2,3}VV$ transitions have been deconvoluted using already proven methods[26] to obtain the transition density of states (TDOS) of clean Al{111}[27] and fully oxidized Al{111} surfaces Al_2O_3.[28] Results are directly comparable to available XPS, UPS, and XES data, and also to theoretical calculations of the DOS. The deconvolution method can also detect surface states in the DOS. Experimental evidence of surface states in Si{111} 7×7 has been reported using this method.[29] Then it is expected that the TDOS obtained self-deconvoluting the $L_{2,3}VV$ Al{111}-25-L O_2 Auger spectrum could be compared with the available theoretical DOS calculation of Salahub *et al.*[25] for this coverage. Moreover, a plot of the Auger amplitudes versus oxygen exposures would allow the identification of the different stages of the process.

II. EXPERIMENTAL

Up to now, all of the oxidation experiments carried out on Al{111} surfaces were made on high-purity single crystals which were polished mechanically and electrolytically.[12,13] However, this polishing seems to affect the properties of the final surfaces,[13] so we decided to prepare our Al samples by vapor deposition on air-cleaved mica in the UHV system. Perfectly oriented single-positioned Al{111} surfaces were obtained at a residual pressure of 1×10^{-8} Torr, substrate temperature of 500 °C, and an evaporation rate of 100 Å/s, the pressure decreasing to 1×10^{-10} Torr after evaporation. A LEED analysis of them[17] showed that they are identical to those obtained from single-crystal Al{111}.[15,16] Moreover, they can always be reconstructed by ion bombardment, annealing at 550 °C, and subsequent Al reevaporation.

Exposures to high-purity 99.999% oxygen were done by introducing the gas into the system through a leak valve without throttling the ion pump at a pressure of 1×10^{-7} Torr, while keeping the substrate at room temperature or 280 °C to reproduce the same experimental conditions of other workers.[3,9,14] The experiments were done in two ways. The first is by stopping the O_2 dosages at different coverages, regaining vacuum (1×10^{-9} Torr), and measuring the Auger peaks and subsequently the *I-V* curves with a spot photometer. The second procedure was to monitor the Auger intensities continuously at the pressure of the oxygen treatment (1×10^{-7} Torr). Both methods give identical LEED and AES results. For Auger analysis we used a primary beam energy of 2000 and 5000 eV, 2 V peak-to-peak modulation amplitude, and a primary beam intensity of 0.1 and 2 μA, respectively. For LEED we used 1 and 0.2 μA, varying the primary electron beam energy in the range 0–170 eV, obtaining similar results. Hence oxygen desorption did not take place during our measurements, nor were electron-stimulated-oxidation (ESO) effects noticed.

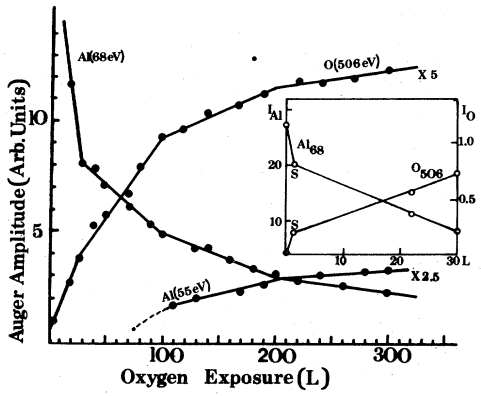

FIG. 1. Al (68 eV), Al (55 eV), and O (506 eV) Auger amplitudes versus oxygen exposures in langmuirs, for RT oxygen adsorption on Al{111} at an oxygen pressure of 1×10^{-7} Torr. Inset is a magnification of the first 30-L O_2 exposure.

III. RESULTS

A. AES

Figure 1 shows a plot of the Auger amplitudes in the derivative mode of Al (68 eV), oxidelike Al (55 eV), and O (506 eV) versus oxygen exposures in langmuirs (1 L = 10^{-6} Torr s) at room temperature and oxygen pressure of 1×10^{-7} Torr. The inset is a magnification of the first 30-L O_2 exposure. Four stages can clearly be distinguished: 0—30 L; 30—100 L; 100—200 L and 200 L onwards. From 0 to 1—2 L there is a very fast decrease of the Al (68 eV) signal. This decrease will be explained in Sec. IV. The variation of the Al (68 eV) Auger transition versus the (506 eV) Auger peak is plotted in Fig. 2. Besides the first fast decrease (dotted line) there are two other breaks at 30 and 200 L which divide the full range of oxygen exposures into three different stages for RT adsorption (curve 1): 2—30 L; 30—200 L, and 200 onwards. Oxygen adsorption at 280 °C is shown by curve 2. Curve 3 represents an oxygen RT adsorption on an annealed (500 °C for 15 h) Al{111} surface exposed to 90-L O_2.

Figure 3 shows the AES low-energy Al spectra and O (506 eV) peak jointly with the corresponding ELS spectra ($E_p=72$ eV), for the points S and T of Fig. 2. Figure 4 shows the transition density of the self-deconvoluted $L_{2,3}VV$ Auger spectrum of

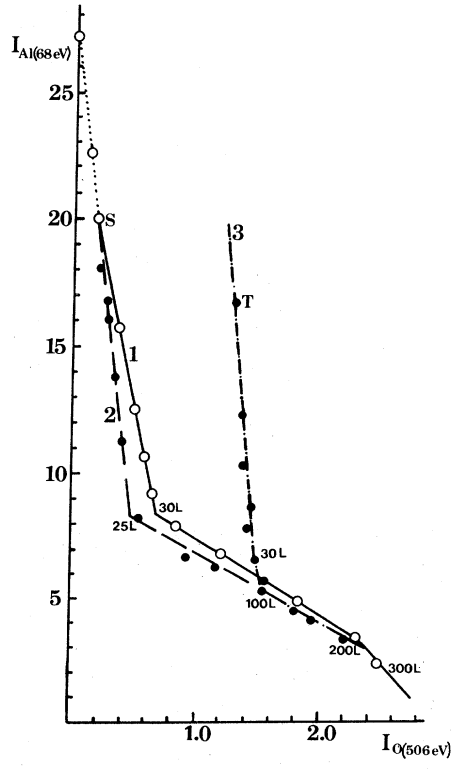

FIG. 2. Variation of the Al (68 eV) versus O (506 eV) Auger amplitudes for oxygen adsorption at RT (1), at 280 °C (2), and at RT on an annealed (500 °C, 15 h) Al{111} after 90-L RT O_2 exposure (3).

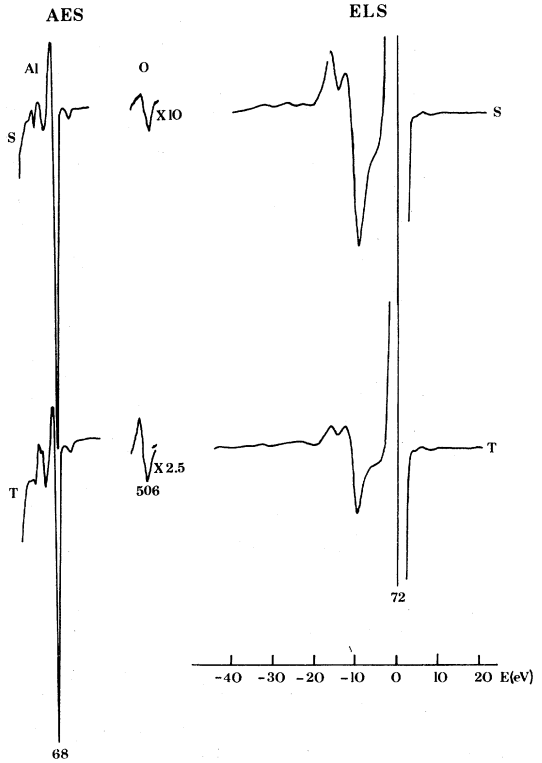

FIG. 3. AES low-energy Al spectra, O (506 eV) Auger peak, and corresponding ELS spectra for points S and T of Fig. 2.

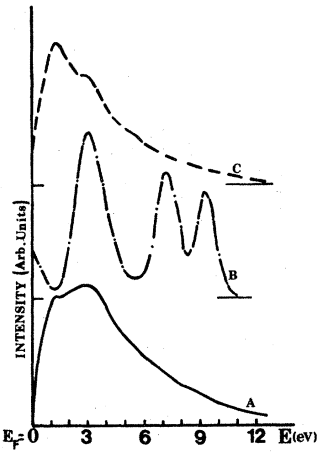

FIG. 4. Transition density of states (TDOS) of the self-deconvoluted $L_{2,3}VV$ Al{111}−25-L O_2 Auger spectrum (*A*); theoretical DOS for oxygen on the threefold fcc hollows of a dilated (10%) Al{111} surface at $d_{12}=0.0$ Å (Ref. 25) (*B*), and experimental TDOS for clean Al{111}surfaces.[27] The curves have been displaced along the vertical axis for the sake of comparison.

Al{111}|for the chemisorption state obtained at an oxygen exposure of 25 L (*A*), and the theoretical DOS obtained for oxygen on a dilated (10%) Al{111} surface occupying the threefold fcc hollow sites at $d_{12}=0.0$ Å (*B*) (Ref. 25). For the sake of comparison the experimental TDOS for clean Al{111} is also included (*C*).

B. LEED

Intensity-versus-energy measurements have been taken at oxygen exposures of 0 (clean surface), 30, 100, and 150 L, at the following incidence angles and beams: (10) and (01), $\theta=0°$ $\phi=0°$; (00), $(\bar{1}0)$, and $(0\bar{1})$, $\theta=5°$ $\phi=18°$; (00) and $(\bar{1}0)$ at $\theta=12°$ $\phi=18°$. This set of beams has been compared to the corresponding theoretical set computed with the CAVLEED[30] package which allows us to treat very close interlayer distances. We have used Al and O potentials constructed following the Mattheiss prescriptions, which assumes overlapping atomic charge, and the Kohn and Sham ($\alpha=\frac{2}{3}$) exchange for Al and Slater ($\alpha=1$) for oxygen. We also used oxygen phase shifts derived from a NiO calculation[31] with identical results. Temperature effects were included by means of eight complex phase shifts. We used the bulk Debye temperature of Al, 428 K, for both Al and O, and muffin-tin radii of 1.43 and 0.73 Å for Al and O, respectively. A constant value for the imaginary part of the self-energy, $V_{0i}=-4$ eV, was used for both Al and O. The "inner potential" V_{0r} was simply determined by shifting the intensity curves until the best agreement was found. Pendry's renormalized forward-scattering perturbation method[32] failed to converge at certain energies, especially for O−Al interlayer distances ≤ 0.9 Å, using in these cases a layer-doubling scheme[33] to calculate the $I(E)$ curves. A maximum of 28 beams and 8 phase shifts were employed, precise numbers being chosen according to energy, using a criterion proposed by Salwen and Rundgren.[34]

We calculated $I_{\text{theor}}(E)$ by varying d_{12} from 0.5 to 1.6 Å at steps of 0.1 Å, the O overlayer following the normal fcc sequence. In order to find the best matching, we used the *R* factor of Zanazzi and Jona,[35] introducing in this way an objective criterion of reliability in comparison with other structure investigations. For the set of seven measured beams at 90-L O_2 exposure, the minimum of the mean r_r factor ($\bar{r}_r$) is 0.22 for $d_{12}=0.7\pm0.1$ Å,

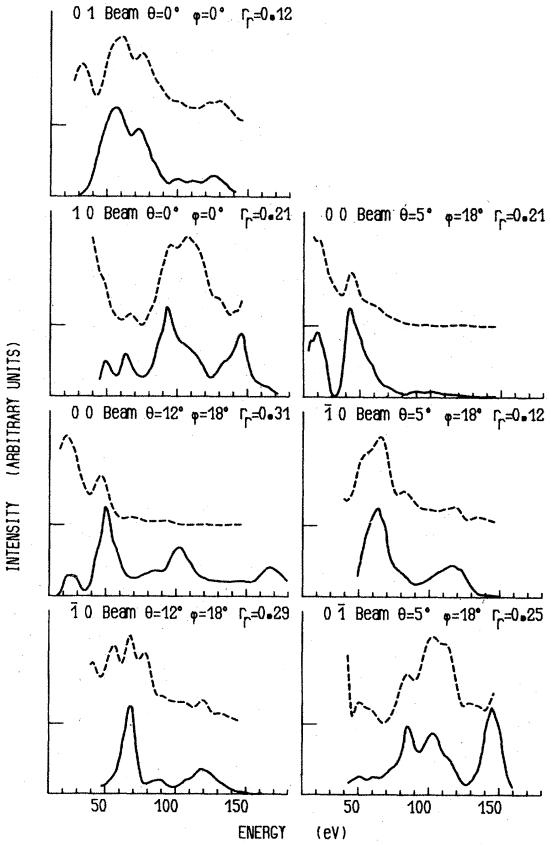

FIG. 5. Experimental (full lines) and theoretical LEED $I(E)$ curves at $d_{12}=0.7$ Å, $V_{0r}=-12.0$ eV (dashed lines) for the Al{111} 1×1-O structure at 90-L RT O_2 exposure.

with $V_{0r}=-12.0\pm0.5$ eV. Figure 5 shows the seven experimental (full lines) and theoretical (dashed lines) beams and the individual r_r factors computed at $V_{0r}=-12.0$ eV. Figure 6 shows $\bar{r}_r$ for the d_{12} spacings of interest. It is interesting to note the two minima at about 0.7 and 1.4 Å, distances already found by SEXAFS[21] and LEED.[5,17,19] The arrow points the best agreement found by Yu *et al.*[17] It is clear from this figure that the best matching occurs between $d_{12}=0.7$ Å and $d_{12}=0.8$ Å, probably at $d_{12}=0.73\pm0.05$ Å, which corresponds to an Al−O distance $d_{\mathrm{Al-O}}=1.80\pm0.02$ Å, in perfect agreement with the SEXAFS result.[21]

Figure 7 shows the experimental and theoretical results for the oxygen (1×1) chemisorbed layer at 150 L. Referring back to the Auger results shown in Fig. 1, we considered the structures at 100 and 150 L to be different from each other, so the earlier LEED results of Yu *et al.*[17] and Martinson *et al.*[5] are not directly comparable, as noted by Jona and Marcus.[36] The mean r_r factors are plotted in Fig. 8, jointly with the mean r factors computed by comparing our theoretical calculations to Martinson *et al.*,[5] experimental results for the (10) and (01) beams at normal incidence. The best agreement is found at 0.8 ± 0.03 Å, with $V_{0r}=-10.5\pm0.5$ eV ($\bar{r}_r=0.21$). The visual agreement found by Martinson *et al.*,[5] indicated by an arrow in Fig. 8, is very poor according to the r-factor value. On the contrary, the agreement for $d_{12}=0.8\pm0.03$ Å is excellent. With these d_{12} spacings, $d_{\mathrm{Al-O}}=1.83\pm0.02$ Å, also in agreement with the SEXAFS results.[21]

IV. DISCUSSION

A. General behavior

If the initial fast adsorption process is not considered, as Fig. 1 shows, the O-Al{111} interaction

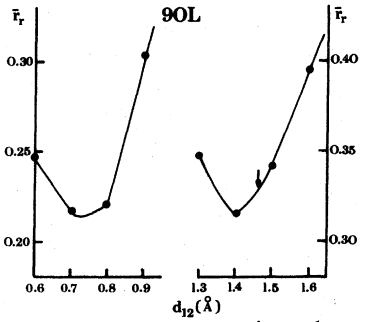

FIG. 6. Mean r_r factor $\bar{r}_r$ versus interplanar distance d_{12} for the Al{111} 1×1-O 90-L structure. The arrow points to the best agreement found by Yu *et al.* (Ref. 17).

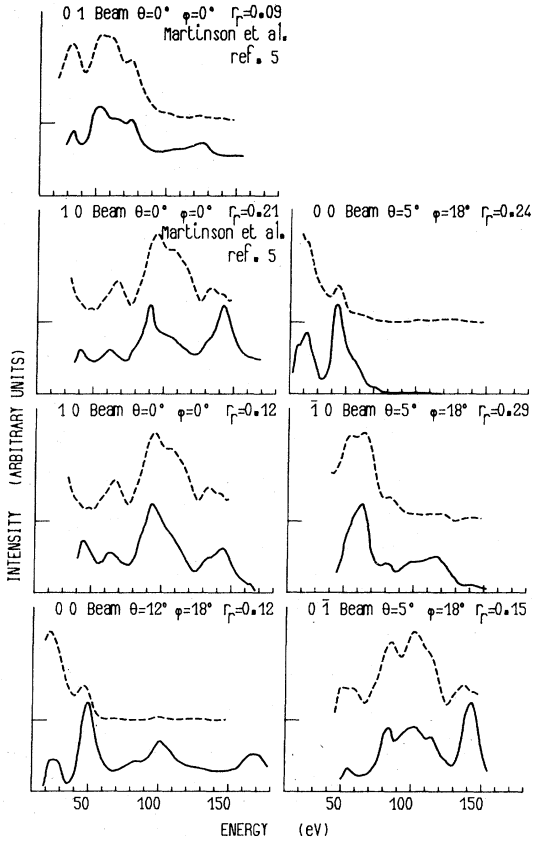

FIG. 7. Experimental (full lines) and theoretical LEED $(I)E$ curves at $d_{12}=0.8$ Å, $V_{0r}=-10.5$ eV (dashed lines) for the Al{111} 1×1-O structure at 150 L RT O_2 exposure.

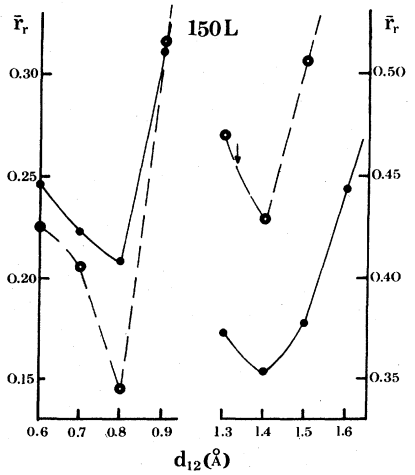

FIG. 8. $\bar{r}_r$ factor versus d_{12} for the Al{111} 1×1-O 150-L structure. Present work, 5 beams (full lines) Martinson *et al.* (Ref. 5), 2 beams (dashed lines). The arrow points to the best agreement of Martinson *et al.* (Ref. 5).

at RT can be described by a four-stage model which accounts for the different experiences and observed phenomena:

(1) 0—30 L. The end of the first stage coincides with the observation of a minimum in $\Delta\phi$,[14] with a break in the AES intensity plot (Figs. 1 and 2) and with the beginning of the appearance of the 1.4-eV shift in the Al $2p$ level.[4]

(2) 30—100 L. During the second stage it is supposed that a chemisorbed oxygen monolayer is completed at 100 L. ARUPS, LEED, and SEXAFS measurements are taken at this coverage. In this interval the 1.4-eV shift peak grows. The Al Auger peaks of lower energy than the main Al $L_{2,3}VV$ show energy variation in the Auger spectrum, although a characteristic Al-oxide peak cannot be detected. $\Delta\phi$ grows, and at about 80—100 L a plateau is reached.

(3) 100—200 L. At these coverages the Al (55 eV) Auger peak characteristic of the oxidelike structure fixes its energy position, and a new 2.7-eV shift of the Al $2p$ level appears. Probably the production of an oxidelike alumina begins, but only for exposures bigger than 100 L. Because of the indetermination in the value of the completeness of the adsorbed oxygen layer, LEED and SEXAFS measurements have also been done at 150 L, although at this coverage some oxidelike alumina is present.

(4) 200—1000 L. In this interval a slow oxidation process takes place, while the adsorbed oxygen layer remains on the surface.

1. Al{111} clean surfaces

In order to understand the first interactions between the incident oxygen atoms and the clean Al{111} surfaces, they have to be completely characterized; this is not trivial. Usually an Al{111} surface is considered clean when the peak-to-peak height of the O (506 eV) signal is less than 1% of the corresponding signal for one monolayer coverage of oxygen,[3,9] less than 0.1%,[8] or less than 0.1 L of oxygen exposure.[7] This purity can be easily achieved by thermal evaporation at pressures below 1×10^{-8} Torr or by ion milling and heating cycles at 550 °C at pressures in the low 10^{-10}-Torr range. Nevertheless, in the figures that show the oxygen adsorption on Al{111} surfaces by AES (Fig. 1 of Ref. 3, Fig. 1 of Ref. 8, and Fig. 2 of Ref. 9), there is more oxygen at 0 L than when the sample was first cleaned. Martinson *et al.*[3] and Gartland[9] find 7—8 % of oxygen at 0 L for the Al{111} surfaces. In the experimental data shown in Figs. 1 and 2 these values are identified by the letters S and T. The existence of this fast adsorption state makes it very difficult to begin the experiments at 1×10^{-7}-Torr O_2 pressure with an oxygen coverage less than 7%, because during the time of increasing oxygen pressure the state saturates. Hence, special care must be taken when the experiments deal with clean Al{111} surfaces. The most reliable method would be to rebuild, *in situ*, the Al{111} surface by thermal evaporation of Al, and to work in the low 10^{-10}-Torr range. Our results for the clean Al{111} surfaces[17,27,28] are in agreement with those of other authors,[16] the amount of oxygen corresponding to this fast adsorption state being about 5—10 % of a monolayer. Henceforth, we can follow the interaction of oxygen with Al{111} by studying in detail each of these four stages.

2. 0—30 L

This is the most controversial range of the oxygen interaction, and there is not a definite model for the adsorption up to 30 L. This stage is characterized by a fast attenuation of the Al (68 eV) Auger peak that cannot be explained by normal quantitative Auger analysis.[37] This strong attenuation is due to surface variations in the structure of the valence band and has also been observed for the chemisorption of oxygen on Si{111} 7×7,[29] and for metal on metal adsorption, as Cu and Ag on Mo{100}, and Ag on W{100} and W{110}.[38]

That AES band transitions are sensitive to these surface states has been experimentally demonstrated by Muñoz *et al.*[28,29] In this stage the UPS spectra present a big resonance at about 7 eV below the Fermi level; this technique is rather insensitive to small structural details near the top of the band in this case.[29] Fortunately, self-deconvoluted $L_{2,3}VV$ Auger spectra indicate a high value in the transition matrix for electronic states near the Fermi level,[29] and the corresponding TDOS can be directly compared to theoretical predictions for different reasonable structures in the preoxidation stages.[25] The comparison between the experimental TDOS obtained by self-deconvolution of the Al $L_{2,3}VV$—25-L, O_2 spectrum and the theoretical calculation of Salahub *et al.*[25] for an oxygen atom in the threefold fcc hollows at $Z=0.0$ Å of a dilated (10%) Al{111} surface is excellent. For the

first time there is experimental evidence of the predicted 3.1-eV peak,[25] not detected by UPS,[7] and also of a small peak at 1.3 eV which has recently been ascribed to Al{111} surface states.[39] As a trade-off the matrix transition elements for 7.2- and 9.2-eV states are very low and only small shoulders are observed. This calculation seems to confirm that the model of oxygen situated on the threefold fcc hollows of a dilated (10%) Al{111} surface is basically correct.

That there is not oxygen diffusion into the Al{111} subsurface for underlayer distances $d_{12}=0.5-1.6$ Å, has been demonstrated by LEED[17] for an oxygen underlayer following the sequence stacking *ACBCABC*. However, the experimental decrease of the $\Delta\phi$ Kelvin measurements (which are directly comparable with the AES and LEED results, while the photoelectric method is not[14]) for chemisorption at RT, suggest a small oxygen incorporation. If this is correct, this incorporation must be smaller than 0.5 Å in the interplanar distances. That the oxygen is situated on a locally expanded (10%) surface is plausible taking into account our results for the Al—O distance ($d_{\mathrm{Al-O}}=1.80\pm0.02$ Å at 100 L and $d_{\mathrm{Al-O}}=1.83\pm0.02$ Å at 150 L). Assuming a hard-sphere radius for the Al atom of 1.43 Å, a radius of 0.38 ± 0.04 Å for the O atom is inferred. If we want to accommodate an oxygen atom of this radius into the threefold hollow we must expand the Al-surface lattice from 2.863 to 3.135 Å, which represents a dilation of 9.5% in excellent agreement with Salahub *et al.*[25] The $\Delta\phi$ decrease can be explained by an electropositive dipole moment in the surface layer and by some roughening of the surface. An electric field with the positive side on the surface has been postulated[40] in order to explain the experimental results of the oxidation of Si{111} 7×7 surfaces with the Cabrera-Mott oxidation theory.[41] Consequently, the idea of a positive surface layer as necessary for the beginning of the oxidation process seems to find another confirmation.

3. 30—100 L

In this region an increase in $\Delta\phi$, which can be associated with the location of the oxygen atoms outside the Al{111} surface layer is observed,[14] and the Al cross-transition (55 eV) Auger peak suffers fluctuations in the peak-to-peak height and energy. From 80 to 100 L the peak moves from 54 to 55 eV, which corresponds in position to one of the Al_2O_3 double-peak energies.[28] This transition is represented by a dashed line in Fig. 1. At around 90—100 L the $\Delta\phi$ shows a plateau, which is an indication that a full oxygen-chemisorbed overlayer stage has been reached. This interpretation of $\Delta\phi$ is strongly supported by LEED and angle-resolved ultraviolet-photoemission-spectrum (ARUPS) measurements. Present LEED results and SEXAFS measurements[21] indicate an Al—O bond distance in this (1×1) overlayer of $d_{\mathrm{Al-O}}=1.80\pm0.02$ Å which corresponds to a vertical interlayer separation $d_{12}=0.73\pm0.05$ Å.

4. 100—200 L

In this range the Al (55 eV) Auger peak starts growing. This peak can be associated with the double peak of fully oxidized Al_2O_3,[28] but its shape is not the same because instead of a double peak only a slight shoulder is visible at 49 eV, where the second peak should be. The chemisorbed (1×1) oxygen layer separates a little, and now the interplanar distance moves from 0.73 ± 0.05 Å at 100 L to 0.80 ± 0.03 Å at 150 L.[42]

This dilation of the Al—O bond distance has also been observed by SEXAFS. Stöhr *et al.*[21] believe that the correct value should be 1.76 ± 0.05 Å at 100 L and 1.81 ± 0.03 Å at 150 L for the chemisorbed oxygen layer, which represents a dilation of 0.15 Å in the interplanar distance (from 0.6 to 0.75 Å). Our LEED results give a dilation of the chemisorbed oxygen layer of 0.07 Å (from 0.73 to 0.80 Å). In our case this value comes from the comparison of the experimental results with a LEED calculation for an oxygen (1×1) overlayer structure. Because the *R*-factor values are comparable with those obtained at 90 L, we inferred that the oxidelike alumina produced must be in a noncrystalline form, producing an increase in the LEED diagram background. Stöhr *et al.*[21] ascribed this oxidelike alumina to the location of oxygen atoms in an underlayer after diffusing through the hcp threefold hollow sites. Despite the small amount of oxide produced, AES and LEED suggest that the overlayer continues along this stage. Figure 2 does not detect a break at 100 L. Then for the Auger electrons the picture is always a layer of O atoms over another of Al atoms. However, Fig. 2 does detect a break at 200 L, which is an indication that another stage does begin. This break can

be seen also in Martinson *et al.*[3] and Michel *et al.* [8] (if we multiply by two the oxygen exposure of these authors,[8] where one monolayer corresponds to 55 L).

Assuming that the completion of the Al{111} 1×1-O overlayer is reached at about 100 L, a mean-free-path value, $\lambda^{O}_{Al_{68}}$, of 2.13±0.21 monolayers (ML) or 3.36±0.34 Å is obtained if a thickness of 0.73 Å is assumed for the Al—O interplanar distance. This value agrees with those found for $\lambda^{Al}_{Al_{68}}$.[43–45] Then it seems that the attenuation of Auger electrons is little influenced by the nature of the overlayer, and the different values obtained for the same transition are within the admitted error in quantitative Auger analysis. Then the coverages for 30 and 200 L will be $\frac{1}{3}$ and 2 ML, respectively. If the monolayer is assumed at about 200 L,[3] the coverages corresponding to 30 and 100 L would be $\frac{1}{6}$ ML, in agreement with Salahub *et al.*,[25] and $\frac{1}{2}$ ML, respectively. The value for $\lambda^{O}_{Al_{68}}$ would then be 1.06±0.1 ML or 0.87±0.09 Å, which is too low. Hence, we favor the completion of the oxygen overlayer at about 100 L, in agreement with the LEED results.

5. 200–1000 L

In this stage the change from the preoxidation to an oxidation Al_2O_3 state takes place. The O (506 eV) peak tends to saturation and the Al (68 eV) tends to zero, while Al (55 eV) tends to the peak-to-peak height corresponding to Al_2O_3. The $\Delta\phi$ curve shows a very small decrease from 200 to 1000 L. Consequently the oxidation process seems to proceed simultaneously in two ways. The chemisorbed layer continues to separate until it reaches an interplanar distance $d_{12}=0.9$ Å which corresponds to $d_{Al-O}=1.88$ Å, which is the distance measured by SEXAFS; and simultaneously, the oxygen in the oxidelike structure occupies both hcp and fcc positions with $d_{12}=0.9$ Å, $d_{Al-O}=1.88$ Å, and $d_{12}=1.16$ Å, $d_{Al-O}=2.02$ Å, destroying completely the crystallinity of the sample. Our $L_{2,3}VV$ Al_2O_3 Auger spectrum[28] is identical to the one identified as anodized Al_2O_3,[46] and its self-deconvoluted $L_{2,3}VV$ spectrum can be compared with XPS and XES experimental results for γ-Al_2O_3.[27] Because the first value of 1.88 Å is identical to the Al—O bond length in spinel-like γ-Al_2O_3, Stöhr *et al.*[21] also conclude that this compound is preferentially formed.

B. Deposition at 280 °C

The effect of temperature consists in a greater attenuation of the Al Auger amplitudes (curve 2 of Fig. 2) for the same O Auger amplitudes, and the formation of the characteristic Al_2O_3 double peak from the beginning of the oxygen dosage. This suggests a thin-film diffusion process rather than a surface-controlled mechanism as happens at RT. Martinson *et al.*[3] observed that if an Al{111} surface covered by 150-L RT oxygen exposure was heated at 250 °C for 8 h, a weaker replica of the original unexposed LEED pattern without any loss in the O (506 eV) amplitude was obtained. We performed a similar experiment after our Al{111} surface was covered by 90-L O_2 exposure at RT. After heating the sample to 500 °C for 15 h, an oxygen adsorption cycle at RT was performed. The results are also shown in Fig. 2 (curve 3). Oxygen adsorption follows the same pattern as at 280 °C, although the whole process is displaced along the abscissa axis. The first point (*T*), Fig. 3, presents an equivalent Al_{68} Auger amplitude to a RT Al{111} surface (point *S*), but with a considerable amount of incorporated oxygen (about 1 ML) which produces the characteristic Al_2O_3 double peak. ELS spectra, in the derivative mode at a primary electron energy of 72 eV, are also shown in Fig. 3 for these two Al{111} surfaces. *T* presents a big attenuation of the Al bulk plasmon at 15 eV with respect to *S*, and an increase of the peak at about 22 eV which can be ascribed to an inelastic transition from the oxygen 2*s* level, 22.5 eV, to an empty level in the proximity of E_F (Fermi energy). These two observations suggest an oxygen incorporation into the Al{111} lattice through at least the first two Al layers. This set of results then shows that thermal oxidation produces oxide nuclei below those two layers, independent of the chemisorption stages.

C. Implications of the LEED and SEXAFS results

The values found by LEED for the O—Al interplanar distance solve the apparent recent contradiction between these two techniques for the Al{111} (1×1)-O system, although the disagreement persists for the Al{111} clean surfaces. Nevertheless, a clear consequence must be inferred from these results: The oxygen radius found by LEED, $r_O=0.38\pm0.04$ Å is, by far, the smallest radius ever found for any O-metal structure

The earlier LEED result $r_O = 0.76 \pm 0.7$ Å was very similar to others found with analogous LEED programs on other surfaces. For instance,

Ni{001}$c(2\times2)$-O $r_O = 0.73$ Å (Ref.47)

Fe{001}$c(2\times2)$-O $r_O = 0.78$ Å (Ref.48)

Co{0001}$c(2\times2)$-O $r_O = 0.70$ Å (Ref.49).

Of these three analyses only the last one[49] has been performed with the aide of the R-factor test. The authors found a mean reliability factor $\bar{r}_r$ of 0.27. If we compare this value with ours (see Fig. 5) for an equivalent oxygen radius, $r_O = 0.73$ Å, $d_{12} = 1.4$ Å, we find an $\bar{r}_r$ value of 0.315. Even in molecules such as CO, the smallest oxygen radius found by LEED is 0.48 Å for the Ti{0001} $p(2\times2)$-CO structure.[50] Now that more sophisticated LEED programs[51] are available, it would be advisable to recalculate some of these structures to see whether this small oxygen radius is only characteristic of the adsorption on Al{111} or is a general phenomenon.

V. CONCLUSIONS

We reach the following conclusions.

(1) The variation of the characteristic Auger intensities of Al, O, and Al_2O_3 shows the existence of a four-stage process for the interaction of oxygen with Al{111} surfaces. The majority of the available experimental data can be phenomenologically interpreted by this four-stage description of the oxidation of Al{111}, several aspects of this interaction being studied in this work.

(2) During the first stage (0–30 L), $\frac{1}{3}$ ML oxygen is adsorbed on Al{111}, producing a strong attenuation of the Al (68 eV) Auger signal which cannot be explained by quantitative AES. A fast oxygen adsorption process in the first 1–2 L has been detected, which accounts for 5–10% of an oxygen monolayer. At 25 L the comparison between the self-deconvoluted $L_{2,3}VV$ Auger transition density of states (TDOS) and the theoretically calculated DOS,[25] provides evidence that at this coverage the oxygen occupies the threefold fcc hollows in an underlayer configuration with an interplanar distance $d_{12} = 0.0-0.5$ Å.

(3) The apparent contradiction between LEED and SEXAFS for the value of the interplanar distance d_{12} between the Al{111} surface and the chemisorbed oxygen (1×1) overlayer has been solved. At 90 L our LEED calculations give $d_{12} = 0.73 \pm 0.05$ Å, and at 150 L $d_{12} = 0.80 \pm 0.03$ Å,[42] in agreement with the values found by SEXAFS.[21] This agreement favors the Salahub *et al.*[25] theoretical calculations for this structure against the Lang *et al.*[22–24] theoretical predictions.

(4) The previous LEED results suggest that it would be advisable to revise earlier LEED interlayer spacing values found in other oxygen-metal systems.

ACKNOWLEDGMENTS

The authors wish to thank D. J. Titterington for a copy of the CAVLEED programs, and Professor Jona for a copy of the R factor. F. Soria acknowledges the Ministerio de Educación y Ciencia, Spain, for financial support. M. C. Muñoz thanks the C.S.I.C. for the provision of a postdoctoral fellowship.

*All correspondence should be mailed to this address.

[1] I. P. Batra and S. Ciraci, Phys. Rev. Lett. 39, 774 (1977).

[2] M. L. den Boer, T. L. Einstein, W. T. Elam, R. L. Park, L. D. Roelofs, and G. E. Laramore, Phys. Rev. Lett. 44, 496 (1980).

[3] C. W. B. Martinson and S. A. Flodström, Surf. Sci. 80, 306 (1979).

[4] S. A. Flodström, C. W. B. Martinson, R. Z. Bachrach, S. B. M. Hagström, and R. S. Bauer, Phys. Rev. Lett. 40, 907 (1978).

[5] C. W. B. Martinson, S. A. Flodström, J. Rundgren, and P. Westrin, Surf. Sci. 89, 102 (1979).

[6] A. Bianconi, R. Z. Bachrach, S. B. M. Hagström, and S. A. Flodström, Phys. Rev. B 19, 2837 (1979).

[7] W. Eberhardt and F. J. Himpsel, Phys. Rev. Lett. 42, 1375 (1979).

[8] R. Michel, J. Gastaldi, C. Allasia, C. Jourdan, and J. Derrien, Surf. Sci. 95, 309 (1980).

[9] P. O. Gartland, Surf. Sci. 62, 183 (1977).

[10] F. Jona, J. Phys. Chem. Solids 28, 2155 (1967).

[11] S. M. Bedair, F. Hofmann, and H. P. Smith, J. Appl. Phys. 39, 4026 (1968).

[12] P. Hofmann, W. Wyrobisch, and A. M. Bradshaw, Surf. Sci. 80, 344 (1979); P. Hofmann, private communication.

[13] A. M. Bradshaw, P. Hofmann, and W. Wyrobisch, Surf. Sci. 68, 769 (1979).

[14] B. Hayden, S. Hachicha, and A. M. Bradshaw, *Proceedings of the 4th International Conference on*

Solid Surfaces and 3rd European Conference on Solid Surfaces, Cannes, 1980, edited by D. A. Degras and M. Costa (Societe Francaise du Vide, Paris, 1980), Vol. II, p. 1125.

[15]D. W. Jepsen, P. M. Marcus, and F. Jona, Phys. Rev. B 6, 3684 (1972).

[16]F. Jona, D. Sondericker, and P. M. Marcus, J. Phys. C 13, L155 (1980).

[17]H. L. Yu, M. C. Muñoz, and F. Soria, Surf. Sci. 94, L184 (1980).

[18]A. Bianconi and R. Z. Bachrach, Phys. Rev. Lett. 42, 104 (1979).

[19]R. Payling and J. A. Ramsey, J. Phys. C 13, 505 (1980).

[20]L. I. Johansson and J. Stöhr, Phys. Rev. Lett. 43, 1882 (1979).

[21]J. Stöhr, L. I. Johansson, S. Brennan, M. Hecht, and J. N. Miller, Phys. Rev. B 22, 4052 (1980).

[22]N. D. Lang and A. R. Williams, Phys. Rev. Lett. 34, 531 (1975).

[23]N. D. Lang and A. R. Williams, Phys. Rev. B 18, 616 (1978).

[24]K. Y. Yu, J. N. Miller, P. Chye, W. E. Spicer, N. D. Lang, and A. R. Williams, Phys. Rev. B 14, 1446 (1976).

[25]D. R. Salahub, M. Roche, and R. P. Messmer, Phvs. Rev. B 18, 6495 (1978).

[26]V. Martínez, J. Electron Spectrosc. Relat. Phenom. 17, 33 (1979).

[27]J. A. Tagle, V. Martínez, J. M. Rojo, and M. Salmerón, Surf. Sci. 79, 77 (1978).

[28]J. A. Tagle, M. C. Muñoz, and J. L. Sacedón, Surf. Sci. 81, 519 (1979).

[29]M. C. Muñoz, V. Martínez, J. A. Tagle, and J. L. Sacedón, Phys. Rev. Lett. 44, 814 (1980); J. Phys. C 13, 4247 (1980).

[30]D. J. Titterington and C. G. Kinniburgh, Comput. Phys. Commun. 20, 237 (1980).

[31]J. E. Demuth, D. W. Jepsen, and P. M. Marcus, Phys. Rev. Lett. 31, 540 (1973).

[32]J. B. Pendry, J. Phys. C 4, 3095 (1971).

[33]J. B. Pendry, *Low Energy Electron Diffraction* (Academic, London, 1974).

[34]J. Rundgren and A. Salwen, Comput. Phys. Commun. 7, 369 (1974).

[35]E. Zanazzi and F. Jona, Surf. Sci. 62, 61 (1977).

[36]F. Jona and P. M. Marcus, J. Phys. C 13, L477 (1980).

[37]C. C. Chang, Surf. Sci. 48, 9 (1975).

[38]F. Soria and H. Poppa, J. Vac. Sci. Technol. 17, 449 (1980), and references therein.

[39]D. S. Wang, A. J. Freeman, H. Krakauer, and M. Posternak, Phys. Rev. B 23, 1685 (1981).

[40]M. C. Muñoz and J. L. Sacedón, J. Chem. Phys. 74, 4693 (1981).

[41]N. Cabrera and N. F. Mott, Rep. Prog. Phys. 12, 163 (1949).

[42]The errors in d_{12} have been estimated from Figs. 6 and 8. Usually the admitted error bars in interlayer distances computed via LEED dynamical analysis are of ± 0.1 Å. To properly estimate these bars, an R factor with statistical significance should be used [J. Pendry, J. Phys. C 13, 937 (1980)].

[43]J. C. Ashley, C. J. Tung, and R. H. Ritchie, Surf. Sci. 81, 409 (1979).

[44]C. J. Tung, J. C. Ashley, and R. H. Ritchie, Surf. Sci. 81, 427 (1979).

[45]C. J. Powell, R. J. Stein, P. B. Needham, and T. J. Driscoll, Phys. Rev. B 16, 1370 (1977).

[46]L. H. Jenkins and M. F. Chung, Surf. Sci. 28, 409 (1971).

[47]P. M. Marcus, J. E. Demuth, and D. W. Jepsen, Surf. Sci. 53, 501 (1975).

[48]K. O. Legg, F. Jona, D. W. Jepsen, and P. M. Marcus, Phys. Rev. B 16, 5271 (1977).

[49]M. Maglietta, E. Zanazzi, V. Bardi, F. Jona, D. W. Jepsen, and P. M. Marcus, Surf. Sci. 77, 101 (1978).

[50]H. D. Shih, F. Jona, D. W. Jepsen, and P. M. Marcus, J. Vac. Sci. Technol. 15, 596 (1978). For a review of LEED-determined oxygen radii, see, for example, F. Jona, J. Phys. C 11, 4271 (1978).

[51]H. D. Shih. in *Proceedings of IBM LEED Structure Determination Conference,* edited by P. M. Marcus (Plenum, New York, 1981).